

Visible-Light-Induced Bactericidal Efficacy of a Platinum-Doped Titanium Photocatalyst

Fereshteh Mohammadi¹, Mohammadreza Nejadmoghaddam¹ and Amir-Hassan Zarnani^{2,3*}

¹Nanobiotechnology Research Center, Avicenna Research Institute, ACECR, Tehran, Iran

²Department of Immunology, School of Public Health, Tehran University of Medical Sciences, Tehran, Iran

³Avicenna Research Institute, ACECR, Tehran, Iran

*Corresponding author: Amir-Hassan Zarnani, Department of Immunology, School of Public Health, Tehran University of Medical Sciences and Avicenna Research Institute, ACECR, Tehran, Iran, Tel: +98 21 22432020; E-mail: zarnania@gmail.com; zarnania@sina.tums.ac.ir

Received date: November 14, 2018; Accepted date: December 06, 2018; Published date: December 13, 2018

Copyright: © 2018 Mohammadi F, et al. This is an open-access article distributed under the terms of the Creative Commons Attribution License, which permits unrestricted use; distribution; and reproduction in any medium; provided the original author and source are credited.

Abstract

TiO₂ photocatalyst has been known to exhibit a notable disinfecting activity against a broad spectrum of microorganisms. Ultraviolet (UV) irradiation is damaging for human chronic contact to UV at the level to excite TiO₂, which is photocarcinogenic. For this study photocatalyst possessing bactericidal activities that could reduce the bacterial population of all tested pathogens when illuminated by visible light was selected. We shifted irradiation wavelength of TiO₂ nanoparticles (NPs) from far UV spectrum to visible (Vis) wavelengths by Platinum (Pt) doping. TiO₂ and Pt-doped TiO₂ (Pt/TiO₂) NPs were synthesized via the sol-gel method in the form of powder and suspension, respectively. XRD, DRS, TEM and SEM techniques and EDX analysis were used to characterize the structure and properties of photocatalysts. Functional activity of both NPs was assessed in vitro by testing bactericidal activity against *Escherichia coli* and methicillin-resistant *Staphylococcus aureus* under UV and Visible irradiation. The results showed that the sizes of TiO₂ and Pt/TiO₂ nanoparticles were in the range of 20 to 50 nm with high crystallinity in the anatase phase. The minimum inhibitory concentration (MIC) of TiO₂ and Pt/TiO₂ NPs was found to be 0.125 mg mL⁻¹. Interestingly, Pt-doping resulted in a marked shift in irradiation wavelength toward Vis spectrum with as almost the same growth inhibition efficacy as TiO₂ at UV irradiation. TiO₂ NPs reduced the growth rate of *E. coli* and *S. aureus* under UV irradiation for 24 hr by 94.3% ± 0.12 and 98% ± 0.16, respectively; while Pt/TiO₂ NPs inhibited growth rate of aforesaid bacterial species at the same time period under Visible irradiation. After 24 hr, growth inhibitory action of Pt/TiO₂ NPs on *E. coli* and *S. aureus* reached to 86% ± 0.11 and 90% ± 0.14, respectively. Taking together, we observed that visible-light responsive platinum-containing titania (Pt/TiO₂) exerted high antibacterial property against pathogenic bacterial strains taken into consideration that apparent quantum efficiency for visible light-illuminated Pt/TiO₂ is relatively higher than titania-based photocatalysts.

Keywords: Bactericide; Nanoparticles; Photocatalyst; Sol-gel; Titanium dioxide

Introduction

A wide variety of active chemical agents exhibit bactericidal activities. Some of the most widely used, including alcohols, iodine, and chlorine, have been employed for a long time in disinfection and preservation [1].

Nowadays, nano metal, metal oxide and their compounds are used widely in antimicrobial application research [2-5], such as Ag [6,7], CdO [8], Fe₂O₃ [9], TiO₂ [10-15], CuO [16], MgO [17], Mg(OH)₂ [18], and ZnO [19,20]. Among nanometal oxides, Photocatalytic titanium dioxide (TiO₂) substrates have been shown to eliminate organic compounds and to function as disinfectants. TiO₂ nanoparticles have been considered in a wide range of applications because of their varied functional potential including photocatalyst, dye-sensitized solar cells, gas sensor and especially in biological and pharmaceutical applications in nanomedicine. These NPs have attracted great interest in their development as potential antibacterial drugs [21,22].

Upon the irradiation of a TiO₂ surface with photons of wavelength ≤ 385 nm, an electron is excited from the valence band to the conduction band, thus forming an electron-hole pair. The photogenerated holes

and electrons react with water molecules attached to TiO₂ surfaces in the presence of oxygen to form hydroxyl radicals and other reactive oxygen species (ROS) such as superoxide ions [23]. It subject of investigation whether these ROS are directly counter parting in bacterial inactivation. Moreover, it remains unclear what conditions of irradiated light necessitate the activation of ROS generation.

Reactive oxygen species (ROS), such as OH[•], O₂⁻ and hydrogen peroxide (H₂O₂) generated on irradiated TiO₂ surfaces, have been shown to operate in concert to attack polyunsaturated phospholipids in bacteria [10]. In addition, it has been shown that photo-irradiated TiO₂ catalyzed site-specific DNA damage via the generation of H₂O₂ [24]. These findings suggested that TiO₂ might exert antimicrobial effects similar to those of the peroxygen disinfectant H₂O₂ [1]. The oxidation of bacterial cell components, such as lipids and DNA, might, therefore, result in subsequent cell death [10].

It has been reported that biophysical interactions occur between NPs and bacteria such as biosorption, NPs breakdown or aggregation, and cellular uptake with effects including membrane damage and toxicity [11,25]. The mechanisms of NPs inhibitory effect on the bacterial growth has been less well understood so far. It has been reported that the size and surface modifications of NPs could affect their antibacterial function [11,23,26].

Several physical and chemical techniques such as sonochemical, hydrothermal, solvothermal, reverse micelles, chemical vapor deposition or light-induced chemical vapor deposition [27], and sol-gel reaction have been used to obtain TiO₂ NPs. Among them, the relatively simple sol-gel method is the most widely used technique due to the advantage of shorter processing time at lower temperatures [28,29].

To enhance the photocatalytic effect in the visible light region, many producing methods were proposed to dope trace impurity in TiO₂ including ion-assisted sputtering, plasma irradiation, ion-implantation, Chemical Vapor Deposition (CVD) and sol-gel. The visible light photoactivity of metal-doped TiO₂ arises from a new energy level produced in the band gap of TiO₂ by the dispersion of metal nanoparticles in the TiO₂ matrix. An electron can be excited from the defect state to the TiO₂ conduction band by a photon with energy equals $h\nu < 3.2$ eV [30-33].

The main purpose of this study was the evaluation of TiO₂ and Pt/TiO₂ NPs efficiency for the inactivation of *Escherichia coli* and *Staphylococcus aureus* bacteria strains. We demonstrated that Platinum-doped TiO₂ substrates have superior visible-light-induced bactericidal activity against two types of bacteria strains compared to the pure TiO₂ substrate. Our data suggest that Pt/TiO₂ is an effective antibacterial photocatalyst which is user-friendly compared to traditional UV-driven TiO₂ photocatalysts.

Materials and Methods

Bacterial strains

Standard strains of *Escherichia coli* (ATCC O55B5) and *Staphylococcus aureus* (ATCC MRSA 25923), as representative gram-negative and gram-positive bacteria respectively, were used in this study.

Chemicals

For the preparation of preliminary TiO₂ suspension, the following materials were used: Titanium tetrachloride (TiCl₄, M=189.79); Nitric Acid (HNO₃, M=63); Ammonia (NH₃, M=17), and Silver nitrate (AgNO₃, M= 169.87). Also, a chloroplatinic acid solution (H₂PtCl₆, 8 wt% in H₂O, M= 409.81) and Ethanol (C₂H₅OH, M=46) were used for the preparation of Pt-doped TiO₂ NPs. All of the materials were obtained from Sigma Chemical Co, USA.

Preparation of anatase TiO₂

In a typical preparation process of TiO₂ nanoparticles, ammonia solution (2.5% v/v) was added dropwise to 20 mL of Titanium tetrachloride (TiCl₄, Merck ≥ 98%) as starting material at room temperature on the magnetic stirrer for an hour to form a suspension with neutral pH. Deionized water was then introduced to the suspension to total volume was reached 500 mL. All additions were accompanied by vigorous stirring for an hour. Ti(OH)₄ suspension was prepared, then washed with deionized water several times to remove the chloride ions. Subsequently, in order to produce a stable sol, this suspension was stirred at room temperature for about 24h and then nitric acid was added dropwise to the mixture until the pH lay between 2 and 3. Therefore, a stable TiO₂ sol was formed. In order to obtain TiO₂ photocatalyst powder, the sol was dried and calcined for 3h at 500°C.

Synthesis of Pt/TiO₂ by photoreduction

100 mg of synthesized TiO₂ NPs was added to 10 mL H₂PtCl₆ of an aqueous metal salt solution (2.5 mmol/L), and then this mixture was dispersed in 200 mL of deionized water in a Pyrex flask under stirring. This flask was exposed to a mercury lamp (125W) for 1.5 h. Then the powder was collected by centrifugation and washed twice by deionized water and ethanol. Finally, the resulting powder was dried at 60°C. The final product had the Pt contents of 0.1%.

Microbiological experimentation

Bacterial strain and growth media: Antimicrobial activity of TiO₂ and Pt/TiO₂ NPs were evaluated using *Escherichia coli* (ATCC O55B5) and *Staphylococcus aureus* (ATCC MRSA 25923), as representative Gram-negative and Gram-positive bacteria strains, respectively. The bacteria strains were grown overnight in a Nutrient-Broth (NB) medium and incubated under aerobic conditions at 37°C with shaking at 250 rpm.

Evaluation of bactericidal effect of TiO₂ and Pt/TiO₂ NPs: Ten µL of each bacteria stock were added to 3 mL NB and cultivated aerobically at 37°C for 24h were then collected by centrifugation at 3000 rpm for 10 min at 4°C, washed three times with 3 ml sterile phosphate-buffered saline (PBS) and resuspended in PBS. Optical density (OD in 600nm) of bacterial suspension was adjusted to 0.1, the cell density corresponding to 106-107 colony forming per milliliter (CFU/ml). Two hundred µl of the suspension was spread onto Luria-Bertani (LB) agar plates whose surfaces had been smeared with 50 µg/ml, 125 µg/ml or 250 µg/ml TiO₂. Culture plates without NP coating served as controls. TiO₂-smeared bacterial culture plates were irradiated with a UV germicidal lamp (15 W) at a constant distance of 54 cm from the plate surface for 10, 20 or 30 seconds. Immediately after UV irradiation, the plates were incubated at 37°C overnight. Optimal concentration and exposure time was then selected based on the maximum growth inhibition rate and applied for exposure of Pt/TiO₂-smeared plates to a visible mercury lamp (125 W) at the same distance mentioned above. All experiments were repeated three times.

Enhancement effect evaluation: Also the antibacterial efficacy of the TiO₂ and Pt/TiO₂ NPs was determined using two shake flask methods; one with NB as the medium, and another with NB and nanoparticles. In the case of the NB test, bacterial growth was monitored by measuring the optical density of the medium over time. The microbial reduction percentage with the TiO₂ and Pt/TiO₂ NPs for both species of bacteria is shown in Tables 4 and 5 respectively.

Result

Chemical analysis

Characterization of the prepared Titanium dioxide and platinum doped to Titanium dioxide nanoparticles was performed with different physicochemical methods. The crystalline structure of TiO₂ nanoparticles was assessed and characterized by X-Ray Diffractometer (XRD D4-BRUKER and Cu-Kα radiation at 30 kv and 20 mA). Also, the Diffuse Reflectance Spectra (DRS Shimadzu-2550) of resulting samples were recorded by UV-Vis spectrophotometer. Morphological studies were carried out using a Scanning Electron Microscope (SEM Philips-XLΦ30 model) and Energy Dispersive X-rays (EDX) analysis. Also, the particle size of the nanoparticles was calculated using

Transmission Electron Microscopy (TEM) was performed with a Jeol JEM- 2100UHR, operated at 200 kV that were previously air-dried.

Antimicrobial activity evaluations

The apparatus for testing the antimicrobial activity was composed of a woody box with a germicidal lamp as UV light source and tungsten lamp as visible light source, a Petri dish as the cover material.

X-ray diffraction

To study the crystallization process and phase identification, X-ray diffraction (XRD) of nano TiO₂ powder was analyzed. As shown in Figure 1 in the X-ray diffraction pattern of TiO₂ powder, peaks were observed at 2θ of 25.18°, 37.88°, and 48.14° which can be indexed as (1 0 1), (0 0 4), and (2 0 0) diffraction planes, respectively. The observed diffraction peaks in recorded XRD patterns correspond to those of the standard patterns of tetragonal anatase TiO₂. No other stable impurity phases were detected in the samples hence prepared materials are fully crystalline. The ratios of peak intensities in prepared powder and that of standard one was the same. The average crystallite size from XRD was calculated from X-ray line broadening of the (1 0 1) diffraction line using the Scherrer's equation ($d = \frac{0.9\lambda}{\beta \cos\theta}$) where d is the grain size, λ is the wavelength of the X-ray (Cu Kα, 0.15418 nm), β is the full-width at the half-height of the peak, and θ is the diffraction angle of the peak. The results were shown in Table 1.

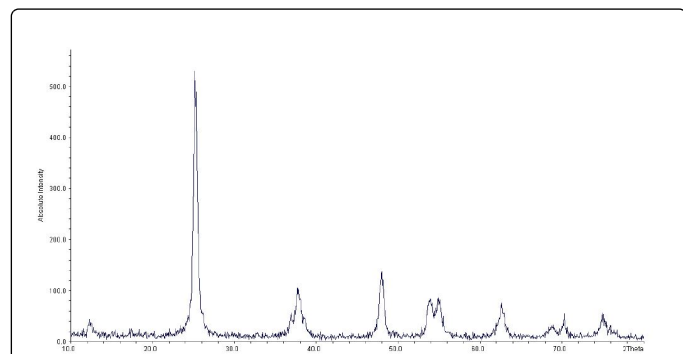


Figure 1: X-ray Diffraction micrograph of TiO₂ powder prepared from preliminary sol after firing at 500°C.

hkl	2θ (°)	d (Å)	The height of the peak
101	25.18	3.53	48.68
-	30.89	2.89	5.19
4	37.88	2.37	10.13
200	48.14	1.88	16.58

"d": The distance between crystalline surfaces
 "θ": diffraction angle of the peak

Table 1: XRD data of TiO₂ nanopowder.

Calculations based on the half-widths of the (1 0 1), (0 0 4), and (2 0 0) diffraction peaks using the Scherrer's formula indicated that the

average size of 30 nm. The symmetry of anatase TiO₂ is tetragonal I41/amd.

Transmission electron microscopy (TEM)

The TEM image of prepared nanoparticles in Figure 2(a), shows that the TiO₂ NPs are single-crystalline with the average size of 25 nm and the surface of the TiO₂ crystals are smooth, while most part of the surface of Pt-TiO₂ crystals is rough, that is shown in Figure 2(b). Meanwhile, with a precise perception in Figure 2 (b), we can realize that there are some fuscous points on the TiO₂ NPs surfaces. Then, Pt has been doped in TiO₂ crystal, but they have poor homogeneity with very irregular shapes and the size range was determined to be between 50 nm to 80 nm.

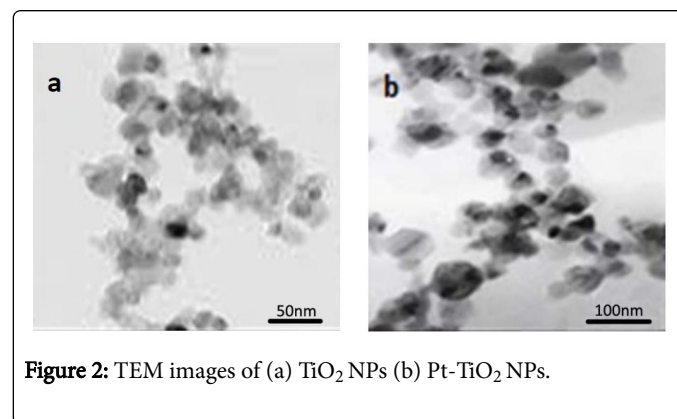


Figure 2: TEM images of (a) TiO₂ NPs (b) Pt-TiO₂ NPs.

Scanning electron microscope (SEM)

The TiO₂ NPs were gold-covered and characterized in the Scanning Electron Microscope (SEM) to investigate their structure and surface characteristic. It was observed that the particles were spherical and were composed of approximately equal size. Nanopowders were homogeneous and fine (Figure 3). It was also possible to find out which elements constructed of a sample by EDX analyze. EDX analysis is the presence of the elements Ti, O, and Pt as presented (Figure 4).

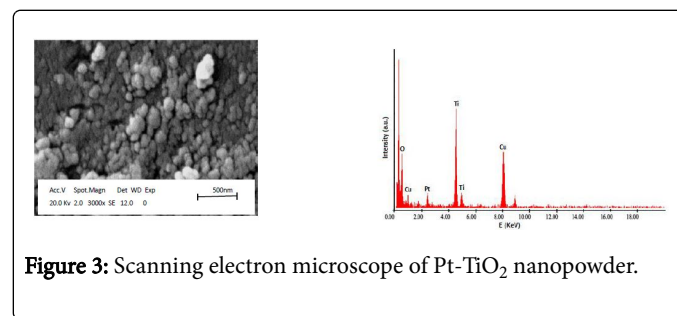


Figure 3: Scanning electron microscope of Pt-TiO₂ nanopowder.

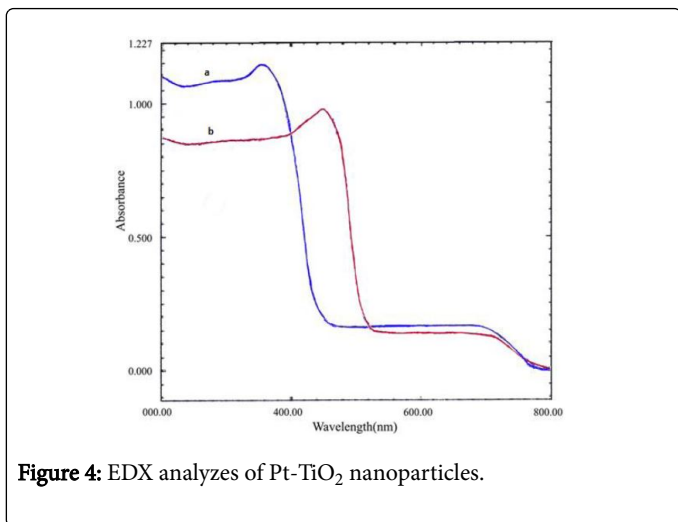


Figure 4: EDX analyzes of Pt-TiO₂ nanoparticles.

UV-visible diffuses reflection spectra (DRS)

The metal TiO₂ doping has been also identified with UV-Visible adsorption spectra. The UV-Visible diffused spectrum of the pure TiO₂ and Pt/TiO₂ nanopowders are seen in Figure 5. It is obviously seen that doping Pt on TiO₂ nanopowder causes bathochromic effect, a shift of a spectral band to higher wavelengths in all the samples doping Pt reveal the redshifts of wavelength, that commonly called redshift absorption edge. This effect has an advantage in lower band gap energy of TiO₂ in other words, lower energy required for electron excitation from the valence band to conduction band. The band gap energy (eV) of each sample were calculated by following ($E = \frac{hc}{\lambda}$) equation (Table 2), where, λ is a cut-off wavelength (m), C is a speed of light (3.0×10^8 m/s), and h is the Planks constant (6.626×10^{-34} Js).

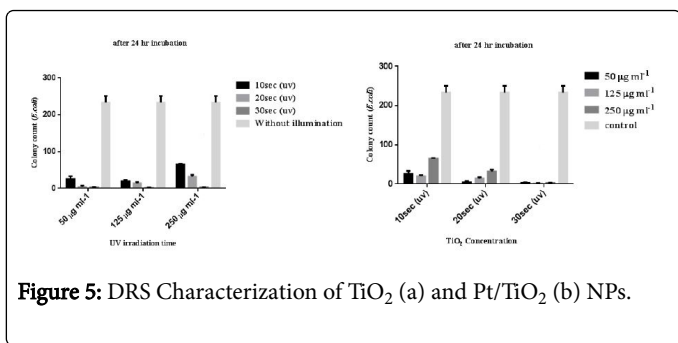


Figure 5: DRS Characterization of TiO₂ (a) and Pt/TiO₂ (b) NPs.

Photocatalyst	TiO ₂	Pt/TiO ₂
Absorbance (nm)	350	450
Bandgap (eV)	3.5	2.7
1eV=1. 602176565e-19 J		

Table 2: Correspondent wavelength and energy bandgap for TiO₂ and Pt/TiO₂ NPs.

Evaluation of photobactericidal effect of TiO₂ and Pt/TiO₂ nanoparticles

The enhancer role of TiO₂ on the bactericidal effect of irradiation (photo bactericidal effect) was quantitatively evaluated by measuring the inhibitory rates (%) of the definite dose of irradiation in presence of various concentrations of TiO₂ and Pt-TiO₂ NPs. The inhibitory rates were calculated by measuring the cell viability through counting the Colony Forming Units (CFU) of *E. coli* or *S. aureus* bacteria on LB agar plates containing TiO₂ NPs after irradiation with UV light and Pt-TiO₂ after irradiation with Visible light (Tests) and also plates without TiO₂ or Pt-TiO₂ and no irradiated (negative controls), using the following formula:

$$GIR (\%) = \frac{100 \times (CFU_c - CFU_T)}{CFU_c}$$

Viable bacterial counts (CFU/ml) after 24h contact time showed log reduction in treated samples compared to the untreated sample. CFU/ml at time zero is 1×10^7 CFU/ml. It was shown that the optimum inactivation of bacteria ($\approx 10^7$ CFU/ml) was achieved in the presence of 0.125 g/L NPs where 99.57% of *E. coli* and 100% of *S. aureus* were inactivated in the best condition. The 0.05 g/L of NPs concentration is insufficient for inactivation reaction of *E. coli* and *S. aureus*. Meanwhile, at 0.25 g/L of NP concentration, it becomes saturated in the suspension, thus give scattering effect in the medium (Table 3 and Figure 6).

Bacteria	Irradiation time (sec)	50 mg ml ⁻¹		125 mg ml ⁻¹		250 mg ml ⁻¹	
		CFU (mean ± SD)	%GIR (mean ± SD)	CFU (mean ± SD)	%GIR (mean ± SD)	CFU (mean ± SD)	%GIR (mean ± SD)
<i>E. coli</i>	10	25 ± 8.736	89.27 ± 0.5057	20 ± 2.516	91.41 ± 0.8576	65 ± 1.527	72.10 ± 0.9136
	20	4 ± 3.605	98.28 ± 0.796	14 ± 3.055	93.99 ± 0.8271	32 ± 4.932	86.26 ± 0.7209
	30	3 ± 1	98.71 ± 0.9434	1 ± 1.527	99.57 ± 0.9136	3 ± 0.577	98.71 ± 0.9673
	0	233 ± 17.677	0	233 ± 17.677	0	233 ± 17.677	0
<i>S. aureus</i>	10	33 ± 2.516	86.69 ± 0.7627	12 ± 3.214	95.16 ± 0.6969	36 ± 4	85.48 ± 0.6228
	20	18 ± 3.214	92.74 ± 0.6969	4 ± 2.516	98.38 ± 0.7627	8 ± 1.527	96.77 ± 0.856
	30	1 ± 0.577	99.59 ± 0.9455	0	100	4 ± 1.154	93.38 ± 0.8911
	0	248 ± 10.606	0	248 ± 10.606	0	248 ± 10.606	0

GIR: Growth Inhibition Rate

Table 3: Effect of different concentrations of TiO₂ NPs on *E. coli* and *S. aureus* viability under irradiation, 24h of incubation.

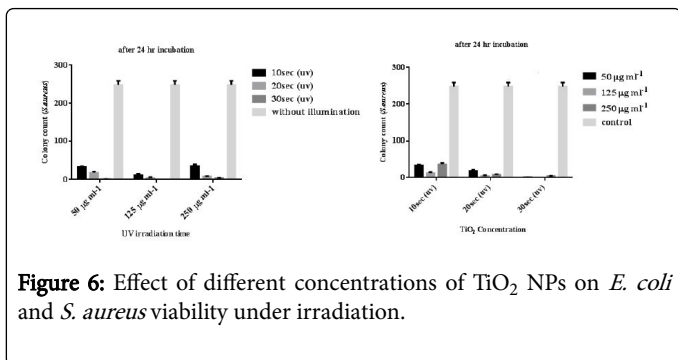


Figure 6: Effect of different concentrations of TiO₂ NPs on *E. coli* and *S. aureus* viability under irradiation.

Also, the antibacterial efficacy of the TiO₂ and Pt/TiO₂ NPs was determined using two shake flask methods; one with NB as the medium, and another with NB and nanoparticles. In the case of the NB test, bacterial growth was monitored by measuring the optical density of the medium over time. The microbial reduction percentage with the TiO₂ and Pt/TiO₂ NPs for both species of bacteria is shown in Tables 4 and 5 respectively.

Test Organism	O.D after 24 hours (in 660 nm)				%Reduction after 30 sec UV irradiation
	Control (Untreated)		TiO ₂ nanoparticles (0.125 mg ml ⁻¹)		
<i>E. coli</i>	2 × 10 ¹⁰	400	1.15 × 10 ⁷	23	94.3
<i>S. aureus</i>	1.2 × 10 ¹⁰	240	2.5 × 10 ⁸	5	98

Table 4: Results of NB shake flask test in terms of growth reduction percentage with TiO₂.

Test Organism	O.D after 24 hours (in 660 nm)				%Reduction after 30 sec Visible irradiation
	Control (Untreated)		Pt/TiO ₂ Nanoparticles (0.1%)		
<i>E. coli</i>	2 × 10 ¹⁰	400	2.8 × 10 ⁷	56	86
<i>S. aureus</i>	1.2 × 10 ¹⁰	240	1.2 × 10 ⁸	24	90

Table 5: Results of NB shake flask test in terms of growth reduction percentage with Pt/TiO₂.

In Figure 7, graphs are included showing the change in absorbance over time. A very high antimicrobial activity was seen against both bacteria.

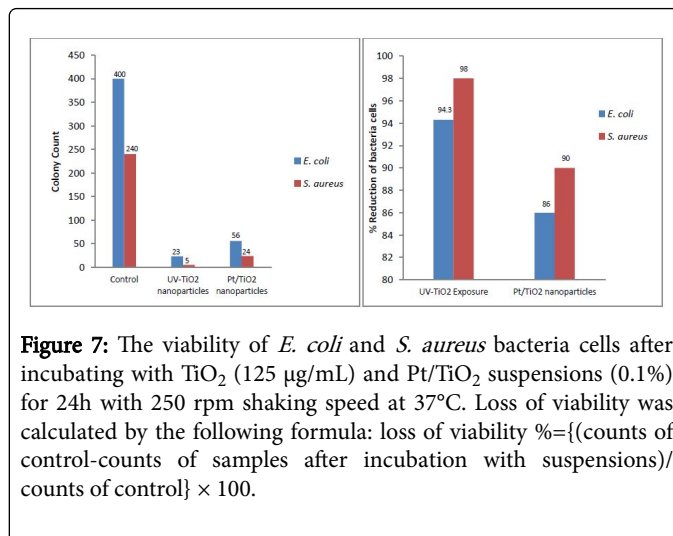


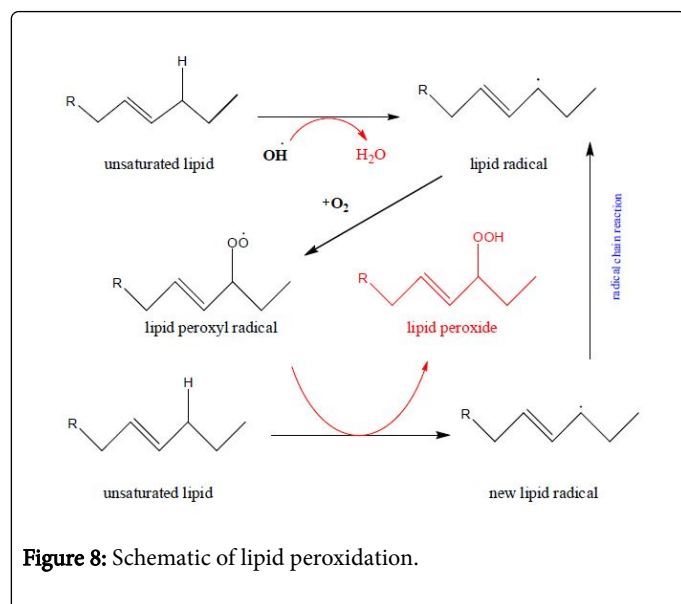
Figure 7: The viability of *E. coli* and *S. aureus* bacteria cells after incubating with TiO₂ (125 µg/mL) and Pt/TiO₂ suspensions (0.1%) for 24h with 250 rpm shaking speed at 37°C. Loss of viability was calculated by the following formula: loss of viability % = {(counts of control - counts of samples after incubation with suspensions) / counts of control} × 100.

Absorbance measurements (Turbidity) are not as accurate as plate counts for the determination of viable bacteria but they can give a rapid estimate of cell numbers and are commonly used for Minimum Inhibitory Concentration (MIC) tests.

Using the absorbance value shown in Tables 4 and 5 after 24h of incubation, there were 94.3% and 86% reduction in growth for *E. coli* with the TiO₂ and Pt/TiO₂ NPs respectively followed by 98% and 90% reduction in growth for *S. aureus*.

Discussion

We have demonstrated that Pt/TiO₂ nanoparticles are effective nanoparticles for inhibiting the cell growth of several pathogenic bacteria under illumination by UV-Visible light. In this study, The TiO₂ and Pt/TiO₂ nanoparticles were synthesized with inorganic substrates by a sol-gel method that showed a very high degree of antibacterial activity when compared to control. Overall the results demonstrated a slightly higher antibacterial activity against *S. aureus* than *E. coli*. Benabbou et al. found that it is possible to increase the percentage of bacterial inactivation by increasing the crystallinity of TiO₂ NPs via calculations as was resulted within the present experiment [34]. In this research, we used TiO₂ crystalline with 100% anatase phase. Sunada et al. found that the mechanism of TiO₂-associated photocatalysis on bacteria could be divided into three stages: Firstly, the outer membrane of the bacteria was attacked and partially decomposed by reactive species such as OH[•], O₂⁻, and H₂O₂; then disordering of the inner membrane leading to the lipid peroxidation threatening cell life; finally, cell death and destruction [35] (Figure 8). According to Fujishima et al. research, if the fluorescent illumination continues for a sufficient time, bacteria will be completely mineralized into CO₂, H₂O, and other mineral components [36].



The visible-light-responsive Pt/TiO₂ NPs can be achieved via a sol-gel method followed by photoreduction. UV curing technique can be applied for activating anatase TiO₂ photocatalytic reactivity of the prepared powder. These powder possess favorable surface properties such as good adhesion, high porosity, and eligible Pt distribution onto the TiO₂ powder. The optimal Pt doping (0.1% mole) to TiO₂ powder provides the synergistic effect on the photocatalytic reactivity. Pt plays a pivotal role in increasing hydrophilicity as well as extending the light absorption spectrum toward the visible region in the benefit of photocatalytic activity. The illumination time required in this approach is shorter than that has been applied in previous studies. Given improvement can be potentially attributed to two main factors. First, optimally sized nanoprobe contributing to the highly efficient energy transfer from UV light to the target bacteria. Second, the targeting capacity of the nanoprobe for several bacteria also results in the effectiveness of the cell growth inhibition of these bacteria. Although the transmission of UV light is limited, this approach should potentially be suitable for the treatment of infections.

Results of the bactericidal investigation indicate that Pt/TiO₂ NPs, as an extremely stable metal-semiconductor nanomaterial, can exhibit a very high photodynamic efficiency under visible irradiation, and our Pt/TiO₂ NPs showed to be relatively effective in the antibacterial property.

Conclusion

In summary, we have presented a facile and efficient synthetic route for the preparation of Pt-doped Titanium dioxide NPs, which has potential applications on the development of an antibacterial material in both in vitro and in vivo settings. In conclusion, the TiO₂ NPs sizes of 20 nm possess significant antibacterial properties against *E. coli* and *S. aureus*. Our results suggested that the TiO₂ NPs have greater efficacy in inhibiting the growth of *S. aureus* compared to the *E. coli* and its inhibitory effects increase as the concentrations of TiO₂ NPs increased. The concluded MIC for *E. coli* and *S. aureus* was 125 µg/mL. The antimicrobial mechanisms of the TiO₂ NPs suggested that oxidation capacity of NPs toward GSH oxidation stress were responsible for antimicrobial behavior of TiO₂ NPs. The results of *E. coli* and *S. aureus* suggest that TiO₂ nanoparticles can be used to

control the growth of pathogenic bacteria. The results from this work are aiding the scale-up of a spray coating process for the production of efficient and economical antibacterial surfaces. Therefore, these surfaces have considerable potential to be recruited in medical instrumentation, water purification systems, hospitals decontaminants, dental office equipment, food storage, packaging, and household sanitation. These findings suggest that Pt-doped TiO₂ has potential application in the development of alternative disinfectants for environmental and medical usages.

Acknowledgment

We are thankful to Avicenna Research Institute for supporting this work.

References

1. Donnell GM, Russell AD (1999) Antiseptics and disinfectants: activity, action, and resistance. Clin Microbiol Rev 12: 147-179.
2. Stoimenov PK, Rosalyn LK, George LM, Klabunde KJ (2002) Metaloxide nanoparticles as bactericidal agents. Langmuir 18: 6679-6686.
3. Hajipour MJ, Katharina MF, Ashkarran AK, Dorleta JA, Idoia RL, et al. (2012) Antibacterial properties of nanoparticles. Trends Biotechnol 30: 499-511.
4. Ameer A, Arham SA, Mohammad O, Mohammad SK, Sami SH, et al. (2012) Antimicrobial activity of metal oxide nanoparticles against Gram-positive and Gram-negative bacteria: a comparative study. Int J Nanomed 30: 6003-6009.
5. Solmaz MD, Farzaneh L, Mohammad BJ, Mohammad HZ, Khosro A (2014) Antimicrobial activity of the metals and metal oxide nanoparticles. Mater Sci Eng C 44: 278-284.
6. Thangaraju N, Venkatalakshmi RP, Chinnasamy A, Kannaiyan P (2012) Synthesis of silver nanoparticles and the antibacterial and anticancer activities of the crude extract of Sargassumpolycystum C. Agardh Nano Biomed Eng 4: 89-94.
7. Tripathi RM, Rana D, Shrivastav A, Singh RP, Shrivastav BR (2013) Biogenic synthesis of silver nanoparticles using Saraca indica leaf extract and evaluation of their antibacterial activity. Nano Biomed Eng 5: 50-56.
8. Bahareh S, Sedigheh M, Mehdi A (2014) Investigation of antibacterial effect of Cadmium Oxide nanoparticles on Staphylococcus aureus bacteria J Nanobiotechnol 12: 26.
9. Prucek R, Tucek J, Kilianova M, Panacek A, Kvitel L, et al. (2011) The targeted antibacterial and antifungal properties of magnetic nanocomposite of iron oxide and silver nanoparticles. Biomater 32: 4704-4713.
10. Pin CM, Sharon S, Daniel MB, Zheng H, Edward JW, et al. (1999) Bactericidal activity of photocatalytic TiO₂ reaction: Toward an understanding of its killing mechanism. Appl Environ Microbiol 65: 4094-4098.
11. Ting MT, Hsin HC, Kia CC, Yu L, Chun CT (2010) A comparative study of the bactericidal effect of photocatalytic oxidation by TiO₂ on antibiotic-resistant and antibiotic-sensitive bacteria. J Chem Technol Biotechnol 85: 1642-1653.
12. Howard AF, Iram BD, Sajnu V, Alex S (2011) Photocatalytic disinfection using titanium dioxide: spectrum and mechanism of antimicrobial activity. Appl Microbiol Biotechnol 90: 1847-1868.
13. Priyanka A, Ganesh K, Suresh G, Anjali R (2015) Synthesis of TiO₂ nanoparticles by electrochemical method and their antibacterial application. Arabian J Chem.
14. Pinggui W, Rongcai X, Kari I, Jian KS (2010) Visible-light-induced bactericidal activity of Titanium dioxide codoped with Nitrogen and Silver. Environ Sci Technol 44: 6992-6997.
15. Michael VL, Erika LB, Vicki LC, Qilin L (2011) Virus inactivation by silver doped titanium dioxide nanoparticles for drinking water treatment. Water Res 45: 535-544.

16. Pramanik A, Laha D, Bhattacharya D, Pramanik P, Karmakar P (2012) A novel study of antibacterial activity of copper iodide nanoparticle mediated by DNA and membrane damage. *Colloids Surf B* 96: 50-55.
17. Osamu Y, Toshiaki O, Kelly A, Fukuda M (2010) Antibacterial characteristics of CaCO₃-MgO composites. *Mater Sci Eng B* 173: 208-211.
18. Dong CX, Song DL, John C, Orville LM, He GH, et al. (2011) Antibacterial study of Mg(OH)₂ nanoplatelets. *Mater Res Bull* 46: 576-82.
19. Raghupathi KR, Koodali RT, Manna AC (2011) Size-dependent bacterial growth inhibition and mechanism of antibacterial activity of zinc oxide nanoparticles. *Langmuir* 27: 4020-4028.
20. Sirelkhatim A, Mahmud S, Seeni A, Mohamad Kaus NH, Ann LC, et al. (2015) Review on zinc oxide nanoparticles: antibacterial activity and toxicity mechanism. *Nano-Micro Letters* 7: 219-242.
21. Irannejada A, Janghorbana K, Tanb OK, Huangb H, Limb CK, et al. (2011) Effect of the TiO₂ shell thickness on the dye-sensitized solar cells with ZnO-TiO₂ core-shell nanorod electrodes. *Electrochimica Acta* 58: 19-24.
22. Robert P, Memarzadeh AK (2014) Nanoparticles and the control of oral infections. *Int J Antimicrob Agents* 43: 95-104.
23. Hashimoto K, Irie H, Fujishima A (2005) TiO₂ photocatalysis: A historical overview and future prospects. *Jpn J Appl Phys* 44: 8269-8285.
24. Hirakawa K, Mori M, Yoshida M, Oikawa S, Kawanishi S (2004) Photo-irradiated titanium dioxide catalyzes site specific DNA damage via generation of hydrogen peroxide. *Free Radic Res* 38: 439-447.
25. Kiwi J, Nadtochenko V (2005) Evidence for the mechanism of photocatalytic degradation of the bacterial wall membrane at the TiO₂ interface by ATR-FTIR and laser kinetic spectroscopy. *Langmuir* 21: 4631-4641.
26. Mori K (2005) Photo-functionalized materials using nanoparticles: Photocatalysis. *KONA* 23: 205-214.
27. Bessekhouad Y, Robert D, Weber JV (2003) Synthesis of photocatalytic TiO₂ nanoparticles: optimization of the preparation conditions. *J Photochem Photobiol A Chem* 157: 47-53.
28. Sharmila Devi R, Venckatesh R, Sivaraj R (2014) Synthesis of titanium dioxide nanoparticles by sol-gel technique. *Int J Innov Res Sci Eng Technol* 3: 15206-15211.
29. Vetrivel V, Rajendran K, Kalaiselvi V (2015) Synthesis and characterization of Pure Titanium dioxide nanoparticles by Sol-gel method. *Int J ChemTech Res* 7: 1090-1097.
30. Zaleska A (2008) Doped-TiO₂: A review. *Recent Patents Eng* 2: 157-164.
31. Chen H, Chen S, Quan X, Yu HT, Zhao HM, et al. (2008) Fabrication of TiO₂-Pt coaxial nanotube array schottky structures for enhanced photocatalytic degradation of phenol in aqueous solution. *J Phys Chem C* 112: 9285-9290.
32. Choi J, Park H, Hoffmann MR (2009) Combinatorial doping of TiO₂ with Platinum (Pt), Chromium (Cr), Vanadium (V), and Nickel (Ni) to achieve enhanced photocatalytic activity with visible light irradiation. *J Mat Res* 25: 149-158.
33. Wong MS, Sun DS, Chang HH (2010) Bactericidal performance of visible light responsive titania photocatalyst with silver nanostructures. *PLoS One* 5: e10394.
34. Benabbou AK, Derriche Z, Felix C, Lejeune B, Guillard C (2007) Photocatalytic inactivation of Escherichia coli, effect of concentration of titanium dioksida and microorganism, nature and intensity of UV irradiation. *App Cat B Environ* 76: 257-263.
35. Sunada K, Watanabe T, Hashimoto K (2003) Studies on photokilling of bacteria on TiO₂ thin film. *J Photochem Photobiol A Chem* 156: 227-233.
36. Fujishima A, Rao TN, Tryk DA (2000) Titanium dioxide photocatalysis. *J Photochem Photobiol C: Photochem Rev* 1: 1-12.